SPATIAL ANALYSIS OF DUST ON SNOW: DUST ORIGIN AND IMPACT IN THE SAN JUAN MOUNTAINS OF SOUTHWESTERN COLORADO

A Thesis

Presented to

The Faculty of the Environmental Program

The Colorado College

In Partial Fulfillment of the Requirements for the Degree

Bachelor of Arts in Environmental Science

By

Henry Hodde

May 2024

Charlotte Gabrielsen

Dr. Charlotte G. Gabrielsen

Assistant Professor of Environmental Science, Colorado College

Jeff Derry

Jeff Derry

Executive Director, Center for Snow and Avalanche Studies

TABLE OF CONTENTS

ABSTRACT

Dust on snow events impact hydrological cycles by decreasing snow surface albedo and increasing the rate of melting cycles for snowpack throughout the spring. This study utilized trajectory modeling and remote sensing to investigate dust dynamics in the San Juan Mountains in southwestern Colorado and greater Colorado Plateau, spanning the Four Corners Region. Using a combination of data from the Center for Snow and Avalanche Studies and Landsat satellite imagery, I characterized the origin of dust storms and infer the resulting impact of dust deposition on albedo and snow extent during two years with dust seasons of varied intensity: 2009 (classified as an average dust year) and 2017 (classified as an extreme dust year).

My findings from HYSPLIT models suggested that in 2009, dust storms typically originated in Arizona, and commonly picked up dust throughout the Colorado Plateau, whereas dust storms in 2017 typically originated from further distances, with two storms originating from California and Mexico. Furthermore, I found that that precipitation may be one potential factor moderating the severity and frequency of dust release. Finally, I found that the greater frequency and intensity of dust storms throughout the 2009 dust season, coupled with average to below average precipitation, led to decreased albedo values throughout the spring, and also increased snowmelt. This study provides an important preliminary step towards better understanding of the impact of dust on snowpack, especially as climate change is likely to result in higher variability in weather and climate, and more extreme winter storms.

ACKNOWLEDGMENTS

I would like to extend a special thank you to my thesis advisor Professor Charlotte Gabrielsen, who helped me extensively throughout the research and writing of this paper. I also would like to thank Jeff Derry of the Center for Snow and Avalanche Studies, who allowed me to travel to Silverton and agreed to work with me for January and February. Thank you to Matt Cooney and all GIS lab techs for their help with geospatial analyses, and to Chris Gober for welcoming me with a place to stay in Silverton. Finally, a thank you to all of my friends and family for supporting me through this process, and to my mother who encouraged me to write this thesis in the first place.

INTRODUCTION

Globally, runoff from snow and glacial melt provides water for nearly 2 billion people (Painter et al., 2018) In the Colorado River Basin, about 70% of streamflow comes from high alpine snowmelt, and this water serves more than 27 million people across the United States and Mexico (Barnett & Pierce, 2009; Christensen et al., 2010). The security of these water resources is crucial in providing an ever-increasing population with the necessary water for their livelihoods and survival. The primary benefit of snowpack in the water equation is that it enables resource storage, whereby melt dynamics drive a strong peak discharge in mid to late spring, followed by a slow regression throughout the summer months, returning to a lower mean streamflow value for the fall and winter (Painter et al., 2018).

Numerous factors contribute to snowmelt. Historically, many attempts to quantify streamflow have focused on response to air temperature measurements, due primarily to the ease of gathering the data (Hock, 2003, 2005). However, correlation between these metrics is weak, as it only considers a narrow portion of the melt equation (Painter et al., 2018). Scientists have found that a stronger indicator for snowmelt is net solar radiation, as it provides the majority of melting energy. For example, in a study conducted in Morteratschgletscher, Switzerland, Oerlemans (2000) found that net solar radiation explained 93% of the net energy flux in the snowpack (Oerlemans, 2000). Similar observations have also been made in Greenland and in the San Juan Mountains of Southwestern Colorado (Painter et al., 2018). When considering the role of net solar radiation on snowmelt dynamics, the two largest contributors include the overall irradiation coming from the sun and albedo – a metric that quantifies the reflectance of the Earth's surface (*i.e.* proportion of incoming solar irradiance that is reflected from a surface; Painter et al., 2018).

The two primary drivers that contribute to the overall reflectance of a snow surface (*i.e.,* albedo) are snow grain size and the presence of impurities. First, the onset of wet snow metamorphism increases grain size, causing a reduction in reflectance in the near-infrared wavelengths (0.8-1.5 nm; Gautam et al., 2013; Painter et al., 2018). This gradual grain growth naturally decreases the albedo of a snowpack with increasing length of time from snow deposition (Gautam et al., 2013; S. M. Skiles et al., 2015). Second, the presence of impurities, such as dust or black carbon deposition, impacts the overall albedo of snowpack through direct and indirect mechanisms. Impurities can directly reduce the albedo by darkening the overall snow surface and in turn, increasing the amount of solar irradiance that is absorbed by the surface (S. M. Skiles et al., 2015; S. M. K. Skiles et al., 2012). Impurities can also indirectly impact albedo, as the snowpack's newfound increased absorption can facilitate further grain growth and cause earlier exposure of a darker underlying substrate (Hansen & Nazarenko, 2003). In combination, these factors can lead to greatly increased solar irradiance absorption for snowpacks in the Southern Rockies, Alps, Caucasus, and Hindu Kush Himalaya mountains, among other mountain ranges (Painter et al., 2018). This increased absorption can significantly impact snowmelt by increasing both the rate and timing of melt cycles. Accordingly, modeling of snowpack melt in any of these regions, without considering the impact of dust and black carbon, may limit researchers' ability to accurately forecast snowpack behavior. Indeed, recent research has highlighted a failure to account for such considerations as a reason for the inaccuracies present in recent Colorado River Basin forecasting (S. M. Skiles et al., 2015).

The San Juan Mountains, located in southwestern Colorado, are particularly prone to impacts from dust deposits. In this region, the mountains are often the first area available for dust deposition when strong, storm-driven southwestern winds kick up dust from the neighboring semi-arid regions of the Four Corners and Colorado Plateau, an area understood to be one of North America's primary dust producers (S. M. Skiles et al., 2015). Dust release in the Colorado Plateau is partly due to human disturbance, with grazing, oil drilling, gas development, and dirt road driving all contributing to a reduced threshold for frictional velocity, in turn causing sediments to become increasingly prone to being picked up and transported by wind (Belnap & Gillette, 1998). While strong dust storms can impact other mountain ranges throughout Colorado, the San Juan Mountains are an ideal study area to characterize the impacts of dust deposition on snowpack because of the frequency of dust events that this region receives. Studies have shown that mountain snowpack in the Colorado River Basin has been impacted by increasing dust buildup – on the order of fivefold or greater – from the Colorado Plateau since the mid 19th century (Neff et al., 2008), and that this loading volume has increased over the past 15 years (Neff et al., 2013). Dust deposition in the San Juan Mountains is most common in the spring (March-June), when winds are highest and conditions in neighboring desert regions are favorable for dust release (S. M. Skiles et al., 2015). Dust events that occur in the spring are also the most influential in accelerating snowmelt, as they coincide with a rising sun angle, greater solar irradiance, and on top of peak seasonal snowpack (S. M. Skiles et al., 2015).

Skiles et al. (2012) investigated the quantitative effect of dust on snow in the San Juan Mountains from 2005-2010 at the Senator Beck Basin Study Site, located east of Red Mountain Pass, and found that springtime dust radiative forcing over the study period ranged from 31–75 W/m^2, and resulted in a decrease in snowpack duration ranging from 21–51 days. Another study by Di Mauro et al. (2019) in the European Alps found that dust and other impurities caused snow to melt prematurely by 11–38 days (Di Mauro et al., 2019). Skiles et al. (2012) also observed that dust led to faster and higher peak discharge values in nearby rivers when compared to dust free conditions, even doubling under the worst dust conditions. Skiles & Painter (2017) also investigated the impact of dust on albedo and found that even minor dust loading initiated a decline in albedo. Furthermore, they discovered that snow depth declined approximately 50% faster in years with higher dust deposition, when compared to years of similar snowfall but less dust.

While dust release in the U.S. Intermountain West has been increasing in frequency and intensity, precipitation can act as a mitigating force by increasing soil moisture. Okin (2022) found that precipitation influenced the potential for dust release by at least 30-40%. When soils are moist, the liquid between the soil particles produces capillary forces, causing them to stick together. This forcing increases the threshold required for dust to be transported in strong wind events. The moisture in the soil is considered to be the most important in the top active layer, which is typically drier than deeper layers (Okin, 2022), and accordingly, the first to be displaced during strong winds. Soil type also has an impact on a moist soil's ability to remain in place; for example, within the top 2 mm, heavy texture soils take approximately half a day to dry, compared to sandier soils which take only about 2 hours to dry (Okin, 2022). Given these soil characteristics, high wind events that are also accompanied by greater precipitation are less likely to result in dust release compared to high wind events that occur after significant time has passed from the date of last precipitation.

While dust deposits in the San Juan Mountains are generally understood to originate from the Four Corners region and the Colorado Plateau, limited understanding of the exact origin locations exists. Several studies have been conducted in an attempt to better understand the regional sources of dust; these studies have utilized particle size and isotopic analysis, remote sensing of dust releases, and backward trajectory analyses (Lawrence et al., 2010; Neff et al., 2008; Painter et al., 2007). While substantial insights have been generated from these studies, uncertainty remains due to mismatches between the spatial and temporal resolution of satellite imagery and the timing and detection of windstorms and dust release. For sensor-based tracking or single point analysis, measurements are typically only available at individual point locations. Accordingly, the ability to assess a larger area without significant extrapolation is difficult.

Objectives

This study utilized trajectory modeling and remote sensing to investigate dust dynamics in the San Juan Mountains in southwestern Colorado and greater Colorado Plateau, spanning the Four Corners Region. Specifically, I used a combination of data from the Center for Snow and Avalanche Studies and Landsat satellite imagery to characterize the origin of dust storms and infer the resulting impact of dust deposition on albedo and snow extent during two years with dust seasons of varied intensity: 2009 (classified as an average dust year) and 2017 (classified as an extreme dust year). The specific objectives of this paper were to (1) model the trajectories of all recorded dust storms from each year to identify their locations of origin; (2) characterize precipitation conditions across the Four Corners Region to infer drivers of dust release; and (3) classify albedo and snow extent from Landsat imagery collected at four time points across each year to infer how alterations to albedo resulting from dust deposition affect the rate of snowmelt across the Northern San Juan Mountains at Senator Beck Basin.

METHODS

Study Area

This research focused on characterizing dust and snow across the San Juan Mountains in southwestern Colorado. The Center for Snow and Avalanche Studies (CSAS) operates four study sites on Red Mountain Pass in the Northern San Juan Mountains (Figure 1). In this study, I focused primarily on the Senator Beck Basin Study Plot (SBSP; 37° 54’ 24.78” N, 107° 43’ 34.56” W), as this area represents the first high-altitude area of contact for predominantly southwesterly winds transporting dust from the southern Colorado Plateau. The SBSP is located on a level bench above tree line in an alpine tundra environment at an elevation of 3719 m. The site has a north/northeast-facing slope of 3˚ and it receives significant wind, providing a representative measurement for much of the surrounding area above tree line (Derry, 2017). SBSP is the most robustly tracked dust-on-snow monitoring site in the United States in terms of both the frequency and duration of monitoring (CSAS, 2024).

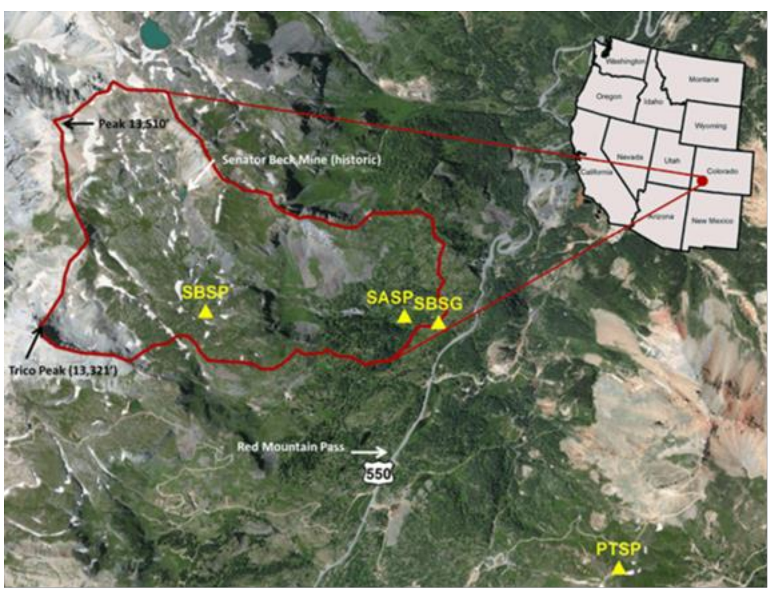

Figure 1. Locations of the four study sites operated by the Center for Snow and Avalanche Studies (CSAS) in southwestern Colorado: Senator Beck Basin Study Plot (SBSP), Swamp Angel Study Plot (SASP), Senator Beck Stream Guage (SBSG), and Putney Study Plot (PTSP).

Dust Season Selection

I assessed the relative impacts of dust deposition on snowmelt in the San Juan Mountains across two separate years with similar snow water equivalent (SWE) and spring precipitation, but varied dust conditions: 2009 – a severe dust season – and 2017 – an average dust season. I selected these two years using matrices developed by CSAS for each year and respective river basin. These matrices contrast total yearly snow water equivalent (SWE), spring precipitation, and dust intensity. According to the CSAS matrix diagrams, both selected years, 2009 and 2017, were classified as high SWE years, defined as having seasons with greater than 110% of the 1981-2010 median SWE on March 1, as recorded by NRCS SNOTEL stations. All six measured Southern Colorado watersheds (Animas River at Durango, Dolores River at Dolores, Rio Grande near Del Norte, San Juan River at Pagosa Springs, San Miguel near Placerville, Uncompahgre near Ridgway) were classified as having high SWE for 2017, and five of the six watersheds were classified with high SWE for 2009 (Rio Grande was classified as having "average" March 1 SWE in 2009). The second axis of the matrix diagrams is a measurement of spring precipitation, with classifications again based on precipitation normals (1981-2010) recorded at NRCS SNOTEL stations. "Average" spring precipitation is classified as any values between 85% and 115% of the recorded median. All six watersheds were classified as "dry" in water year 2017, while four of the six stations received "dry" classifications for 2009 (Rio Grande and San Juan stations were classified as receiving "average" spring precipitation). Finally, dust classifications in the matrix diagrams are based on CSAS measurements since monitoring began in 2005. All six watersheds were classified as having “average dust” intensity in 2017; in contrast, all six watersheds were issued a “maximum dust” classification in 2009 (CSAS, 2024).

Both 2009 and 2017 water years (1 Oct 2008 – 30 Sept 2009, and 1 Oct 1 2016 – 30 Sept 2017, respectively) were high snow years. In 2009, early winter produced strong snowfall, which was accompanied by exceptionally strong winds, leading to two dust events before the new year. Water year 2009 also experienced abnormally high temperatures and low precipitation in March. The first half of May was generally dry and sunny for the San Juan Mountains; however, following mid-month, rain became a daily occurrence, and temperatures cooled. Peak SWE at Red Mountain Pass SNOTEL was recorded at 27.5” on April 19. All snow was gone by May 23 (Table 1). Notably, the time between peak SWE and snow all gone was just 36 days across 15 monitoring sites throughout Colorado – which represents the third shortest duration of time since data collection began in 2005 (Figure 3). Dust in 2009 was widely considered to be one of the worst in memory, with 12 observed events (Table 3). The sixth, seventh, and eighth dust events of the year (Mar 22, Mar 29, and Apr 3, respectively) were considered to be particularly extreme.

Water year 2017 produced above average precipitation and experienced large temperature fluctuations. October and November 2016 exhibited little to no precipitation and very warm temperatures. During December to February, however, snowfall was abundant, resulting from several atmospheric rivers that occurred throughout the winter (Figure 2). March 2017 was the warmest March on record, which continued into the beginning of April. Cold and stormy weather returned at the end of April, lasting through early June. Snow water equivalent peaked at 30” on April 26, and snowpack was observed to have fully melted at the study site by June 13 (Table 1). Finally, four dust events were observed throughout the 2017 water year at Senator Beck Basin

Study Area at Red Mountain Pass (Table 4). The Colorado Dust-on-Snow (CODOS) Project, classified the 2017 dust season as being on the lighter side of average.

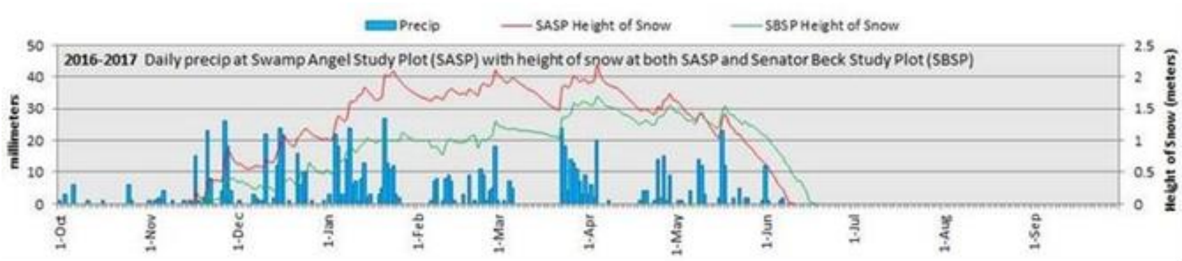

Figure 2. Daily seasonal precipitation amount (mm) at the Swamp Angel Study Plot and snow height (m) at the Senator Beck Study Plot (SBSP) over the course of water year 2017, (1 Oct 2016 – 30 Sep 2017). Graph courtesy of CODOS.

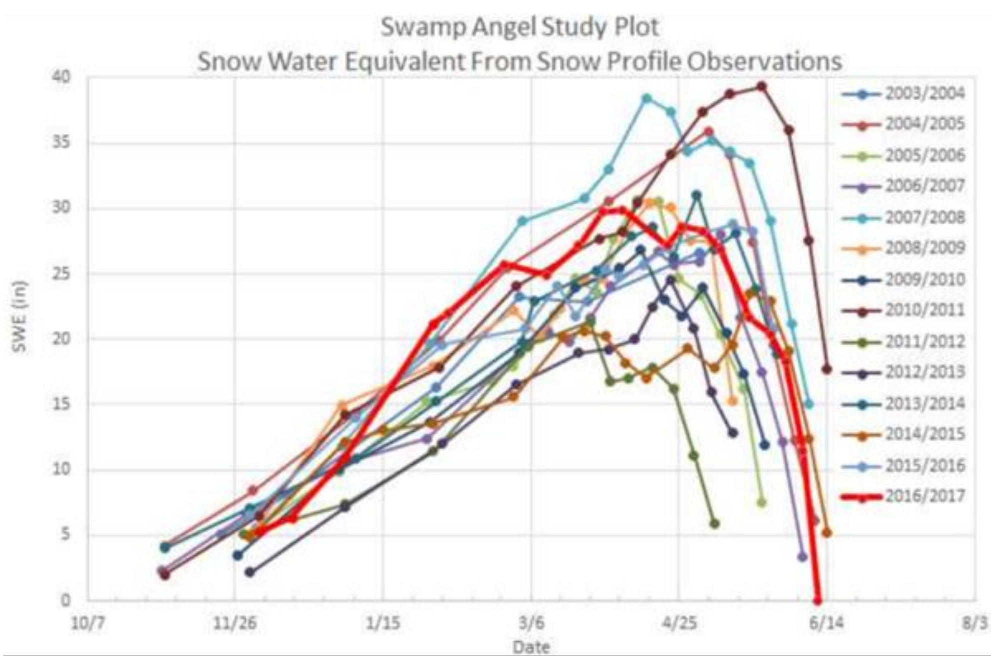

Figure 3. Snow water equivalent (SWE) recorded at the Swamp Angel Study Plot from the 2004-2017 water years. Graph courtesy of CODOS.

Table 1. Number of dust events, estimates of SWE from Red Mountain Pass (maximum, date of peak, adjusted daily mean loss), snow all gone (SAG) date, and mean temperature across each selected water year (2009 and 2017). (CSAS, 2009; Derry, 2017)

		SWE				
Year	# of dust events	max (in)	date of peak	adj. daily mean loss	SAG date	mean temp (˚C)
2009	12	27.5	4/19/09	0.79	5/23/09	4.3
2017	4	27.4	4/05/2017	0.5	6/13/17	0.2

HYSPLIT Modeling to Identify Dust Sources

To identify the origin of the dust storms that deposited dust across the study area, I used the HYSPLIT model developed by the National Oceanic and Atmospheric Administration (NOAA; Stein et al., 2015)The HYSPLIT model tracks air particle trajectory and dispersion through the atmosphere using a combination of the Lagrangian approach, which performs diffusion and advection calculations, and the Eulerian approach, which employs a three-dimensional grid to calculate concentrations (Stein et al., 2015). The HYSPLIT model is one of the most commonly used meteorological tracking systems, and has been used for numerous applications, including wildfire smoke detection, volcanic ash monitoring, dust distribution, and pollutant and hazardous material tracking (Stein et al., 2015). The model can calculate single particle trajectories, or it can apply matrix and grid-based calculations to assess movement of a larger area of air. Scientists have updated and improved the model considerably since launching the software in 1949 (Figure 4). I used the HYSPLIT model to calculate back trajectories, a process aimed at tracking the history of air particle movement before it arrives at a particular location. Back trajectories can be calculated for different lengths of time depending on the period of relevance, with this particular model offering up to 7 days of back trajectory tracking. Particle tracking is useful for understanding overall atmospheric motion as the motion of one particular particle often provides a good representation of the storms and phenomena dictating its movement.

To visualize the storm tracks for each dust event, I used HYSPLIT to model back trajectories spanning 24 hours from the date of all listed dust storms in 2009 and 2017. I ran all back trajectories so that they ended at the Senator Beck Basin Study Plot. I ran the back trajectories using the normal trajectory option, as I was interested in tracking single particles that ended up at SBSP, rather than a matrix, ensemble or frequency trajectory. Furthermore, I chose one finishing location (as opposed to multiple) and ran the GDAS (1 degree, global, 2006-present) option for the meteorology option on the setup page as this included both selected study years, and also produced a sufficiently acute resolution for my analyses. I modeled the vertical velocity over a duration of 24 hours, as this allowed for sufficient understanding of general air movement during that period while also encompassing a long enough duration to detect potential changes in the trajectory of each storm track. Particles were measured at an atmospheric height of 500 meters above ground level. I exported all of the resulting trajectories as shapefiles and imported them into ArcGIS Pro for visualization.

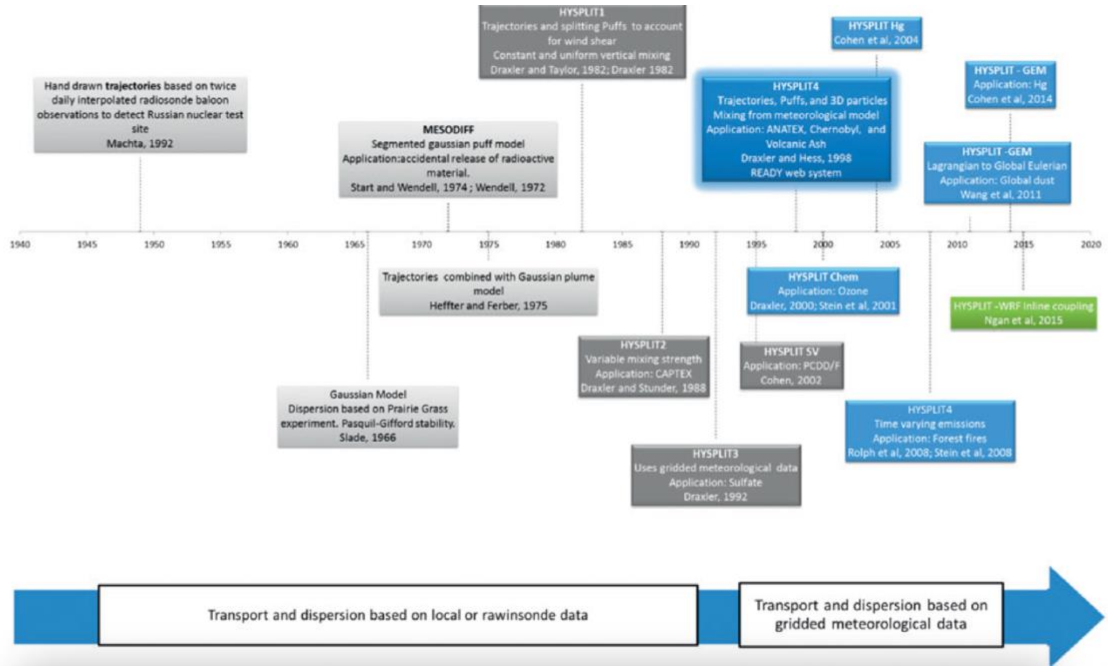

Figure 4. Timeline displaying improvements to the HYSPLIT trajectory model since its initial development in 1982 (Stein et al., 2015).

In addition to modeling the origin of dust using HYSPLIT models, I used wind roses to further understand how the dust was arriving at SBSP. The CSAS keeps a log detailing wind speed, gust and direction at each of their monitoring sites. Through the CSAS website, I logged the primary wind direction, average wind speed, and max wind gust speed for each of the dust events that occurred during 2009 and 2017. I also was able to acquire wind roses for each of these events to observe the wind speeds occurring from each direction.

Precipitation Departure from Normal

Because precipitation is the best-known metric for predicting the occurrence of dust transport via wind, I characterized precipitation conditions across the Four Corners Region, which comprises Arizona, New Mexico, Colorado and Utah. I downloaded 4-km spatial resolution PRISM monthly gridded precipitation data (PRISM Climate Group, Oregon State University) for January through May of 2009 and 2017. As precipitation is known to aid in dust retention irrespective of whether it falls in the form of snow or rain, I used raw precipitation data rather than distinguishing precipitation separately by its form. Next, I used the raster calculator in ArcGIS Pro to generate a sum of total precipitation accumulated over a five-month period from January through May of each year. I selected these five months as this is when dust events are most common and when precipitation is most impactful in preventing dust release.

To provide a reference to a historic baseline, I also downloaded 30-year normals for precipitation at 4-km spatial resolution, which represent precipitation conditions over the most recent three full decades (1991–2020). For the precipitation normals, I downloaded average monthly precipitation data from five months (January through May). Similar to above, I produced a normal dataset, producing a normal precipitation raster layer through those five months based on 1991-2020 data. Next, I subtracted the normal raster layer from the 2009 and the 2017 layer to produce departure maps for both of these two years. Finally, I clipped the raster using a polygon of the four corners states, aiming to focus exclusively on the areas that most commonly release dust.

Classification of Albedo and NDSI from Landsat

To characterize albedo and snowpack extent in the San Juan Mountains, I classified Landsat satellite imagery collected during the 2009 and 2017 dust seasons. Landsat imagery has a moderate spatial resolution of 30 meters, which provided sufficient resolution to determine changes over relatively small differences in area across the large spatial extent of the study area, compared to MODIS (250-1000 m resolution). I used Landsat-5 Thematic Mapper (TM) imagery to classify albedo and snow extent in 2009 and Landsat-8 Operational Land Imager (OLI) imagery for 2017. I selected Landsat imagery from four time points across for each year (January, March, April, May) to visualize changes in albedo and snowpack extent across the dust season (Table 2).

Table 2. Summary of Landsat imagery attributes associated with each of the classified scenes from 2009 and 2017 (n=8 Landsat scenes total).

Year	Date	Path/row	Landsat Sensor	Cloud cover (%)	Sun elevation (degrees)	Spatial resolution
2009	01/16/09	35/34	TM	0%	26.51	30 m
2009	03/05/09	35/34	TM	1%	40.02	30 m
2009	04/06/09	35/34	TM	1%	52.07	30 m
2009	05/08/09	35/34	TM	0%	61.55	30 m
2017	01/06/17	35/34	OLI	0.41%	26.62	30 m
2017	03/11/17	35/34	OLI	1.87%	43.80	30 m
2017	04/12/17	35/34	OLI	4.16%	55.78	30 m
2017	05/14/17	35/34	OLI	12.19%	64.54	30 m

To calculate albedo for each Landsat scene, I first calibrated the digital number (DN) values of each Landsat image using the Apparent Reflectance function in ArcGIS Pro. The calibration uses sun elevation, acquisition date, sensor gain and bias for each band to derive Top of Atmosphere (TOA) reflectance, plus sun angle correction. Next, I calculated albedo from the reflectance rasters using the Liang (2000) equation below, as the formula has been shown to provide good estimates for mean albedo values for glaciers (Naegeli et al., 2017) and snow covered surfaces (Hammar et al., 2023).

$$\alpha = \frac{0.356\rho_1 + 0.130\rho_3 + 0.373\rho_4 + 0.085\,\rho_5 + 0.072\rho_7 - 0.0018}{0.356 + 0.130 + 0.373 + 0.085 + 0.072}$$

In this equation, ρ_1 corresponds to the blue band (band 1 for Landsat 5, or band 2 for Landsat 8); ρ_3 corresponds to the red band (band 3 for Landsat 5, or band 4 for Landsat 8); ρ_4 corresponds to the near infrared band (band 4 for Landsat 5, or band 5 for Landsat 8); ρ_5 corresponds to the SWIR 1 band (band 5 for Landsat 5, or band 6 for Landsat 8); and ρ_7 corresponds to the SWIR 2 band (band 7 for both Landsat 5 and Landsat 8).

Next, I used the normalized difference snow index (NDSI) as a proxy to assess snow extent across the study area throughout the melt season (January – May) across each of the Landsat scenes for both years (2009 and 2017). NDSI is particularly useful for separating snow from vegetation, soils, and lithology and is calculated as the normalized difference between the green (G) and the shortwave infrared (SWIR 1) band, using the equation below:

$$NDSI = {(G - SWIR\ 1)}\big/{(G + SWIR\ 1)}$$

The resulting index, which ranges from -1 to 1 represents the probability that snow is present in a given pixel.

Statistical Modifications

To enable inferences about the effect of dust on snow on albedo and the spatial extent of snowpack, I generated statistical summaries of the albedo and NDSI rasters across each of the four time points in both years. For these summaries, I limited the spatial extent of the study area to only the area covered with snow as defined by the maximum snow extent in March across both years. By doing so, I removed data from lower elevation areas that do not typically hold snow, and where bare ground and exposed rock could make it difficult to make inferences about albedo variations due to dust on snow alone.

Next, I reclassified the NDSI rasters using a threshold of 0.3, where NDSI values ≥ 0.3 were classified as snow, and values < 0.3 were classified as snow-free. From the resulting binary snow raster, I used ArcGIS Pro to calculate the proportion of snow covered and snow free pixels at each time point across both 2009 and 2017. I also calculated statistics for albedo, again limiting the spatial extent of the snow area as I did for the NDSI maps. Finally, I generated statistical summaries to calculate the mean and standard deviation of NDSI across all images from each year.

RESULTS

Dust Origin

The HYSPLIT models suggested that in 2009 (the year characterized as having a severe dust season), dust storms typically originated in Arizona, and commonly picked up dust throughout the Colorado Plateau, an area characterized by arid, desert like conditions (Figure 5a). Storms in 2009 typically approached from the southwest, arriving at an angle between 198° and 326°, with a mean of 223.92° (Table 3). Average wind speed ranged from 17.2–50.4 mph with a mean speed of 28.77 mph, and maximum wind gusts ranged from 60.3–107.6 mph, with a mean speed of 74.95 mph. In contrast, dust storms in 2017 typically originated from further distances, with two storms originating from California and Mexico. The remaining two dust storms originated in Northern New Mexico and Central Arizona (Figure 5b). Storms in 2017 typically approached from the southwest, arriving at an angle between 183° and 228°, with a mean of 206° (Table 3). Average wind speed ranged from 23.9–40 mph with a mean speed of 31.4 mph and maximum wind gusts ranged from 61.3 mph–81.8 mph, with a mean speed of 68.42 mph (Table 3).

Table 3. Summary of data derived from wind rose plots associated with each dust storm event date in water years 2009 and 2017.

Water Year	Date	Dust Event	Primary Wind Direction (˚)	Average Wind Speed (mph)	Max Wind Gust (mph)
2009	10/11/08	D1	198	50.4	107.6
	12/13/08	D2	227	33	65.2
	2/27/09	D3	326	17.2	62.5
	3/6/09	D4	211	31.6	71.9
	3/9/09	D5	214	33.8	77.6
	3/22/09	D6	250	24.1	79.9
	3/29/09	D7	240	27.4	75.7
	4/3/09	D8	206	33	72.9
	4/8/09	D9	223	29.7	70.6
	4/15/09	D10	164	20.4	60.3
	4/24/09	D11	214	22.3	77.6
	4/25/09	D12	214	22.3	77.6
		Mean	223.92	28.77	74.95
2017	3/5/17	D1	218	40	81.8
	3/23/17	D2	195	32.6	66.6
	3/31/17	D3	183	23.9	64
	4/9/17	D4	228	29.1	61.3
		Mean	206	31.4	68.42

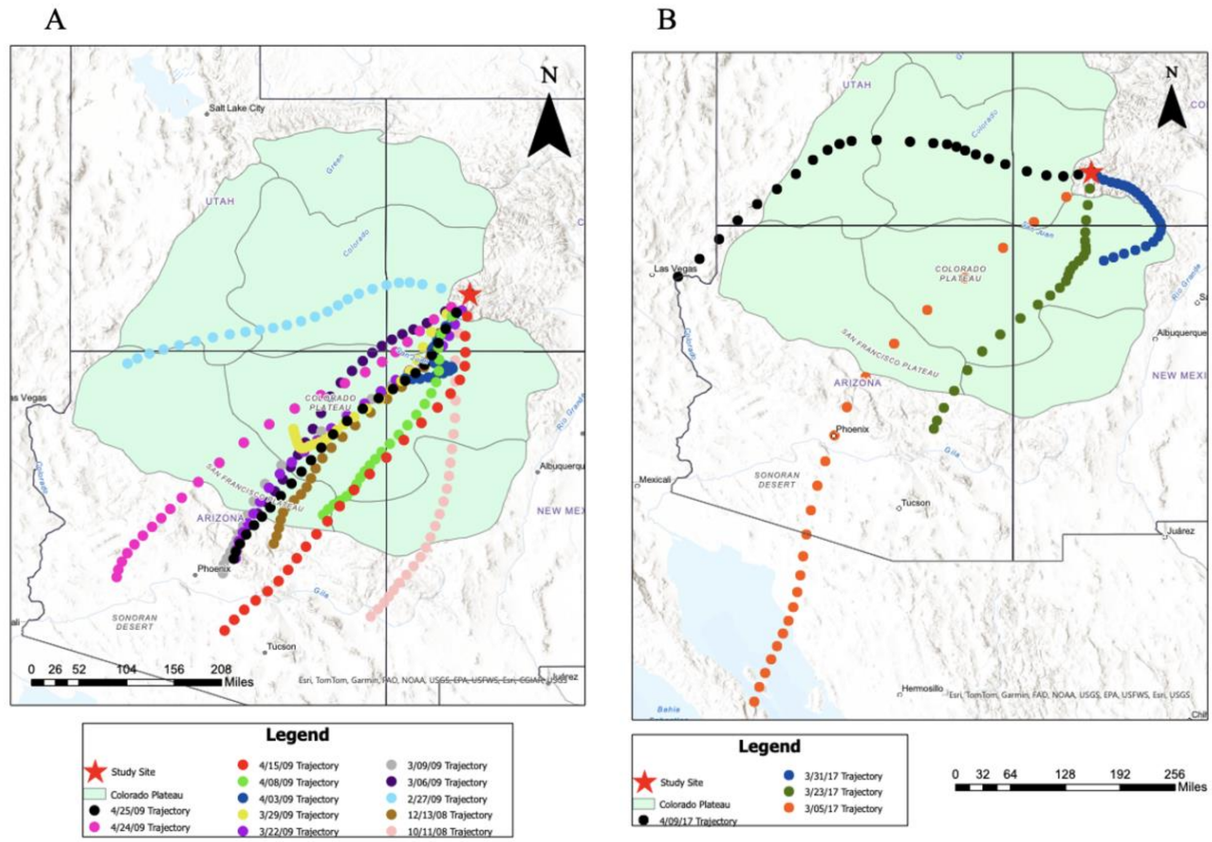

Figure 5. Trajectories for all dust storms occurring during (a) 2009; and (b) 2017. Individual points along each storm backward trajectory represent 1-hr time intervals spanning 24 hours prior to arrival at the Senator Beck Study Plot.

Precipitation Departure

Precipitation during the period from January–May 2009 was, for the majority, similar to the historical baseline, especially within Utah and Colorado, whereby most areas received precipitation within 50 mm of the median precipitation for the area, and other areas, such as in much of Arizona and New Mexico, received precipitation less than the median value (Figure 6a). Some isolated areas received more precipitation than the median normal precipitation amount;

these areas were primarily high elevation areas such as portions of the Wasatch Mountains of Utah, and some mountainous areas of Colorado – notably the Flat Tops Range near Steamboat Springs, and portions of the Elk Mountains of Central Colorado. Conversely, precipitation during spring 2017 was generally at or above historical baseline measurements across the Four Corners states, especially across Utah and Colorado (Figure 6b). Much of Colorado received higher than normal precipitation, including mountainous areas and a significant portion of the Eastern Plains. The northern half of Utah generally received higher precipitation than normal, especially throughout the Wasatch Mountains. Very few, if any, areas experienced precipitation below the 30-year historical median (1991-2020).

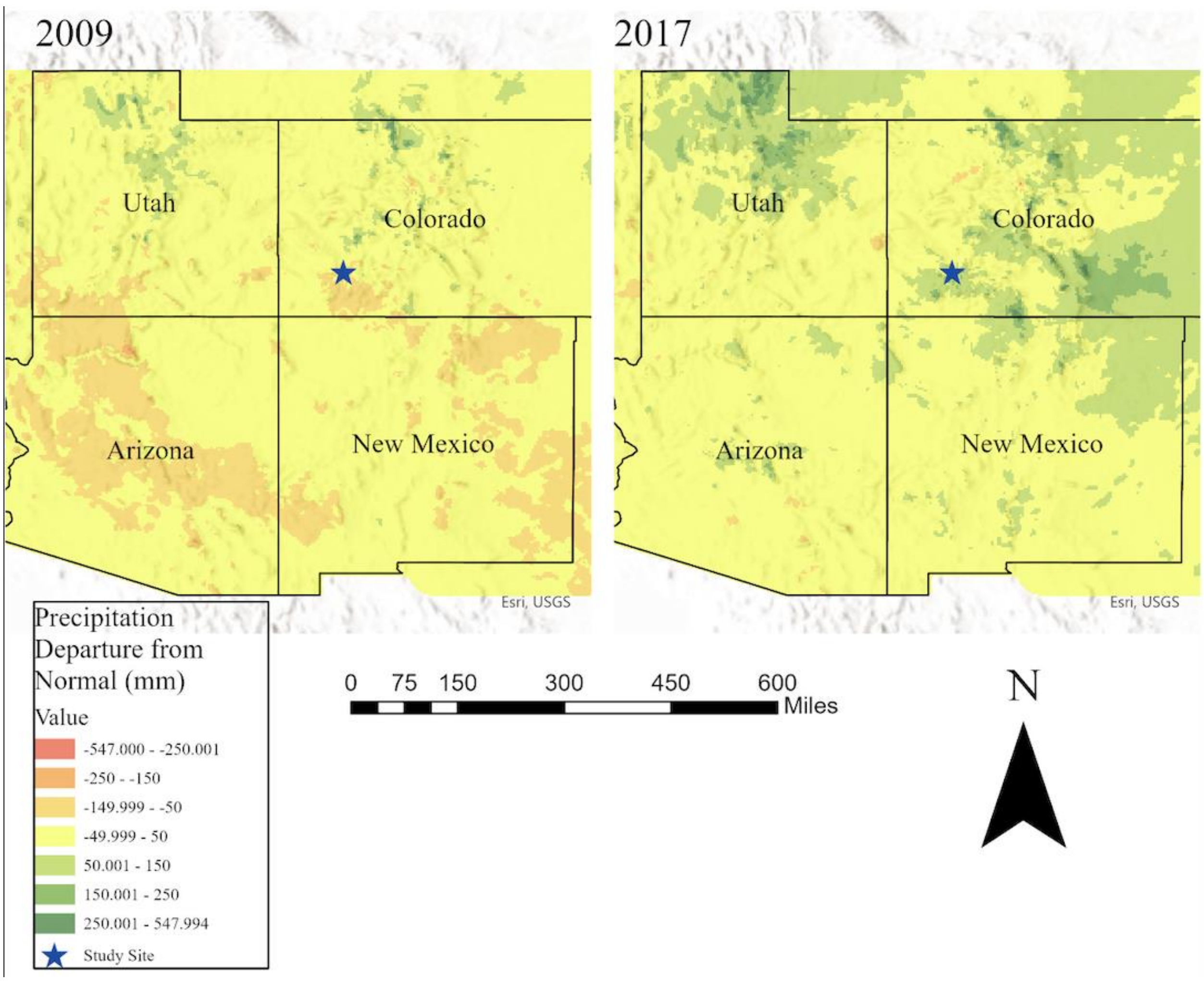

Figure 6. Precipitation departure from normal (1991-2020) conditions in (a) 2009 and (b) 2017 across the Four Corners Region.

Dust Deposition

In both years, albedo declined with each progressive time step throughout the melt season, and this remained consistent through the maps (Table 5). However, mean values of albedo were higher across all four time steps in 2017, compared to 2009, whereby mean albedo was 0.14 higher in January 2017 than January 2009, 0.12 higher in March, 0.04 higher in April, and 0.06 higher in May (Table 5). The maps show a similar pattern, with a strong preference for red and orange throughout all four time steps. This is especially prevalent at the highest elevations (between Silverton and Ouray). The notable exception is at lower elevation areas in April (Figure 7c), where albedo values are higher in 2009 (green colors). Conversely, variability in albedo, as measured via standard deviation, was higher in 2017, where values were larger than 2009 across the time steps (differences ranging from 0.05–0.12; Table 6).

Table 6. Mean and standard deviation of albedo for each time point (n=4) across the 2009 and 2017 dust seasons. The total area analyzed (defined by the maximum snow extent in March) was 11,100 km^2.

Year	Month	Mean Albedo	Standard Deviation
2009	January	0.35	0.18
	March	0.26	0.14
	April	0.24	0.13
	May	0.13	0.12
2017	January	0.49	0.3
	March	0.38	0.23
	April	0.28	0.22

May	0.19	0.17

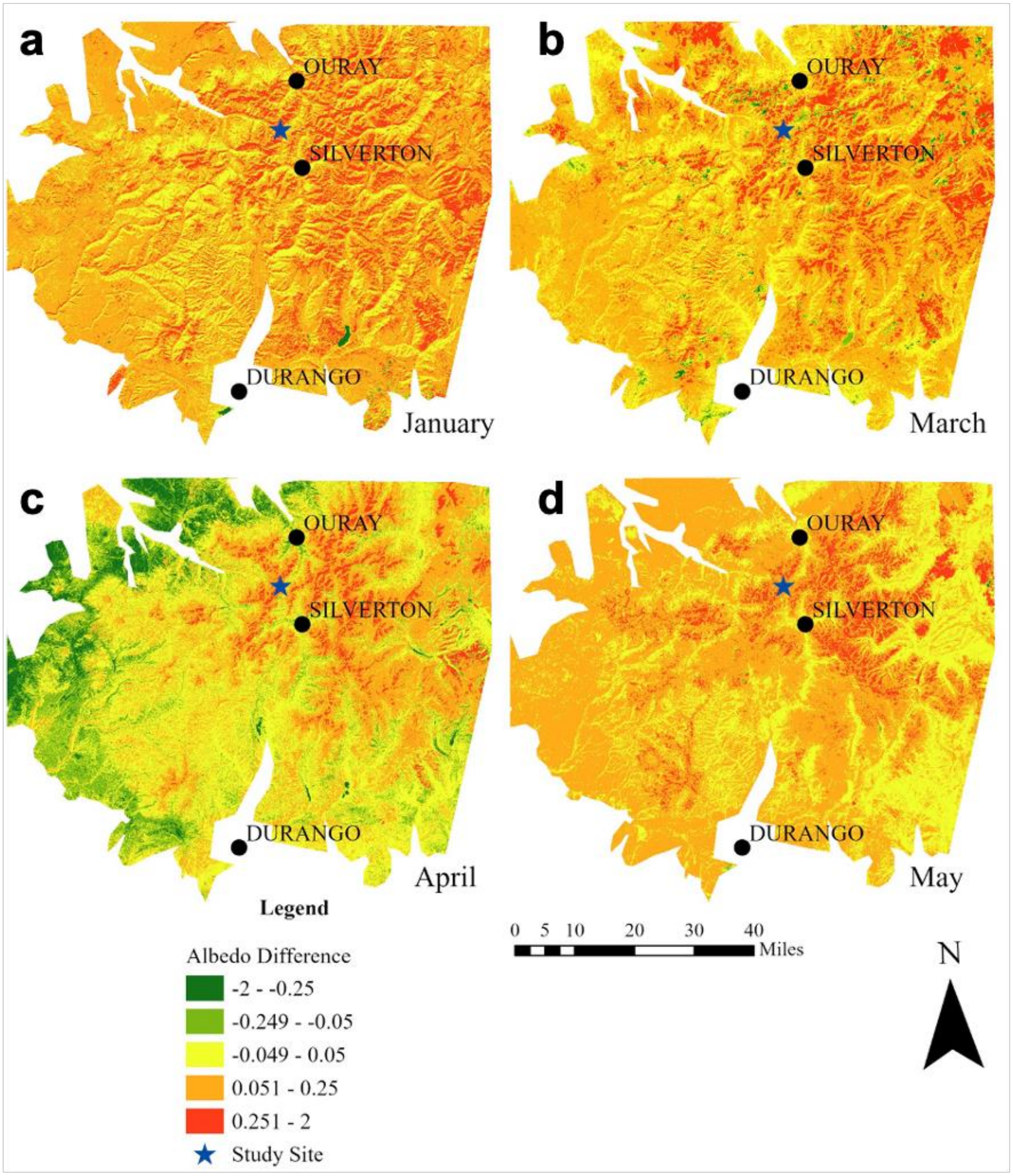

a
OURAY
SILVERTON
DURANGO
January
b
OURAY
SILVERTON
DURANGO
March
c
OURAY
SILVERTON
DURANGO
April
d
OURAY
SILVERTON
DURANGO
May
Legend
Albedo Difference
-2 - -0.25
-0.249 - -0.05
-0.049 - 0.05
0.051 - 0.25
0.251 - 2
Study Site
0 5 10 20 30 40
Miles
N

Figure 7. Change in albedo between 2009 & 2017 for the months of (a) January, (b) March, (c) April, and (d) May. Negative values, in green shades, indicate where NDSI values were comparatively higher in 2009; positive values, in orange and red, indicate where NDSI values were higher in 2017. Yellow areas, centered on values of zero, indicate areas where NDSI was relatively similar in both years.

Snow extent, derived from values of NDSI with values ≥ 0.3, was similar for the month of January in both 2009 and 2017, with snow covering 54% and 63% of the designated study area, respectively (Figure 8a). However, as the snowmelt season progressed, I observed that the percentage of snow declined 7%, 19%, and 18% across each progressive timestep in 2017 whereas the percentage of snow across the 2009 snowmelt season declined by 8%, 1%, and 32% across each time step (Table 6). By observing the difference maps, I found that higher elevation areas tended to trend towards orange and red, suggesting that snow cover was more widespread in 2017 than in 2009. Lower elevation areas shifted to green and yellow, suggesting that snow cover in these areas was more widespread in 2009 than in 2017 (Figure 8). While mean albedo remains consistently higher throughout each calculation in 2017 as compared to 2009, I observed different trends in the decline of snow fraction across the two years of analysis (Figure 9). In 2009, very little melt occurred initially, followed by a significant decline in the percentage of snow between April and May. In contrast, I observed more consistent declines in the percentage of snow and less fluctuation over the course of the melt season in 2017.

Table 6: Statistical summaries of snow and snow-free area (m^2) and percentage of snow for each time point (n=4) across the 2009 and 2017 dust seasons. The total area analyzed (defined by the maximum snow extent in March) was 11,100 km^2.

Year	Month	Snow extent (m^2)	Snow-free extent (m^2)	Snow Percentage
2009	January	5.95E+09	5.14E+09	54%
	March	5.09E+09	6.00E+09	46%
	April	4.98E+09	6.10E+09	45%
	May	1.43E+09	9.65E+09	13%
2017	January	6.93E+09	4.13E+09	63%
	March	6.16E+09	4.92E+09	56%
	April	4.10E+09	6.99E+09	37%
	May	2.10E+09	8.99E+09	19%

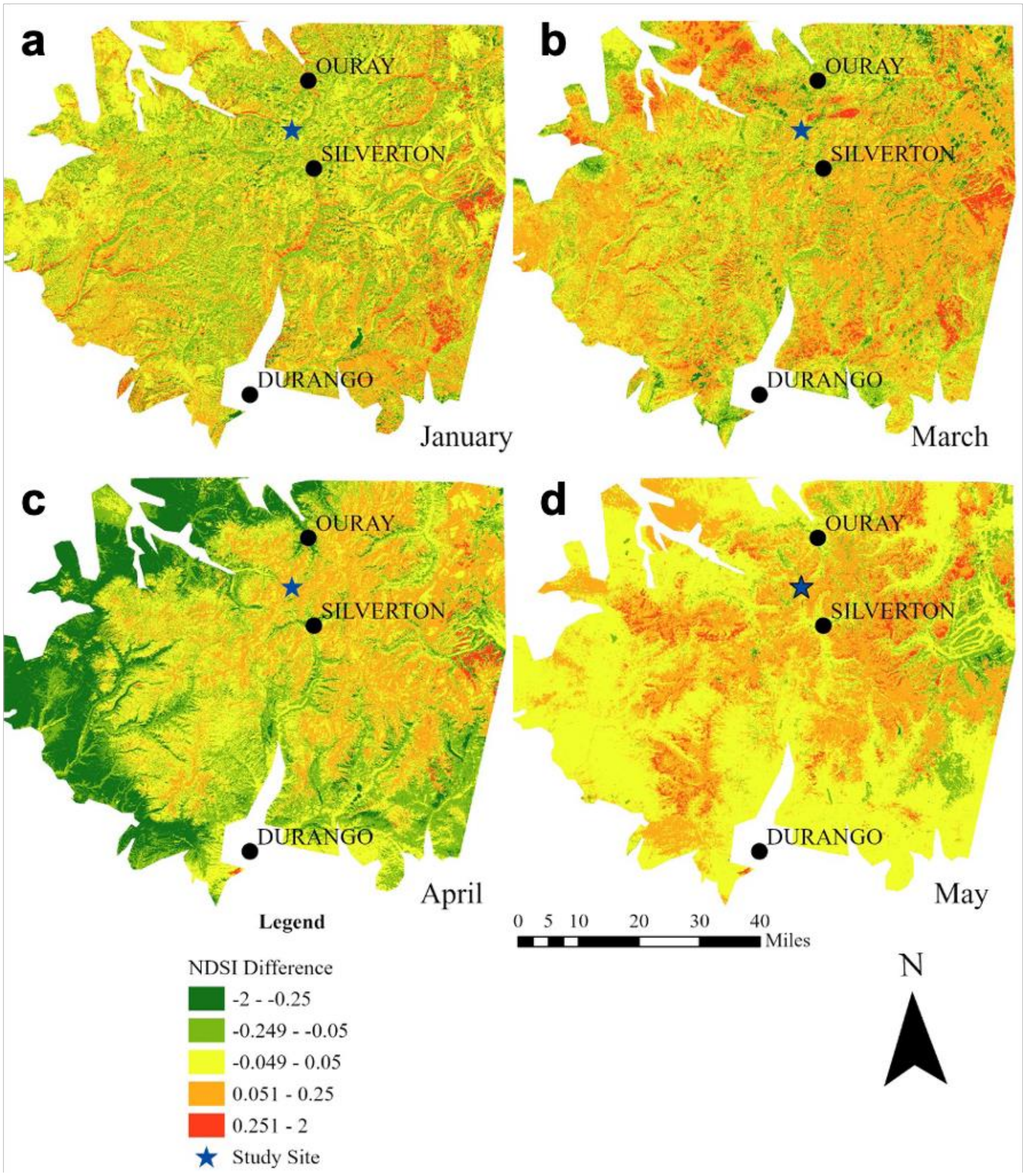

Figure 8. Change in normalized difference snow index (NDSI) between 2009 & 2017 for the months of January (a), March (b), April (c), and May (d). Negative values, in green shades, indicate where NDSI values were comparatively higher in 2009; positive values, in orange and red, indicate where NDSI values were higher in 2017. Yellow areas, centered on values of zero,

indicate areas where NDSI was similar in both years.

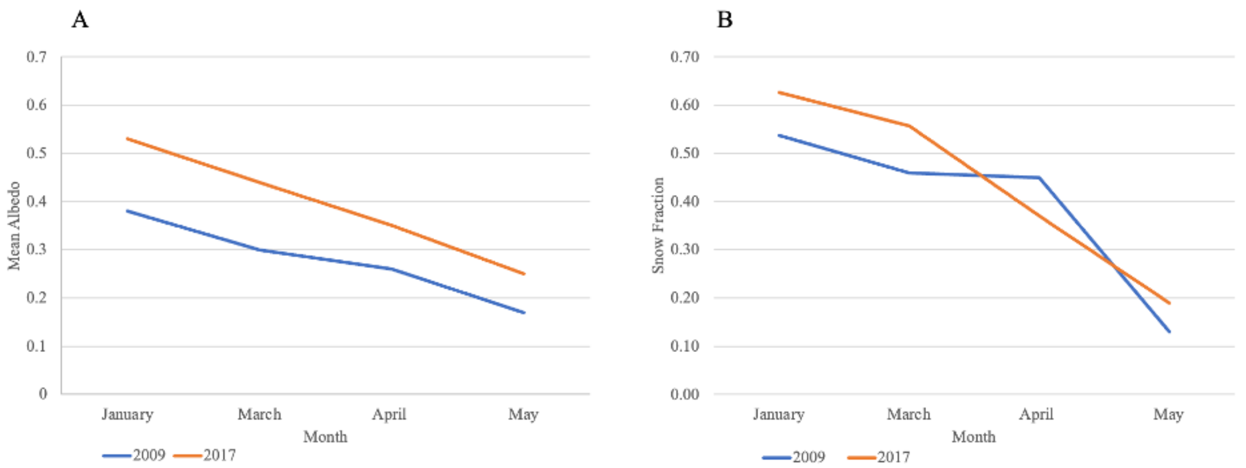

Figure 9. Trends in (a) mean albedo and (b) snow fraction (proportion of snow-covered pixels for 2009 and 2017.

DISCUSSION

Dust Storm Origins & Trajectories

In 2009, the majority of dust storm trajectories (11 of 12 total dust storms) tracked through northeastern Arizona or northwestern New Mexico, or a combination of both (Figure 5a). The exception to this trend was the trajectory of D3, which occurred through southern Utah on February 27, 2009. The mean wind direction from the wind rose data collected at Senator Beck Study Plot of 223.92˚ is consistent with the overall trajectories modeled with HYSPLIT (Figure 5a). In 2017, three of the four dust storms passed through northeastern Arizona or northwestern New Mexico, whereas one storm tracked a more northerly route through southern Utah (Figure 5b). Similar to 2009, the wind rose data aligned with the inferences drawn from the modeled HYSPLIT trajectories; the mean wind direction was 206˚, meaning that most wind arrived at the study plot from the southwest, with a slight skew towards the south-southwest direction compared to a more west-southwest track (Table 3). Overall, while more of the 2009 storms arrived at SBSP directly from the southwest, it is important to note that there were only four dust storms in 2017 and so, the small sample size may limit the ability for strong inferences to be made. Finally, wind speeds were generally faster during 2017 dust storms than those that occurred during 2009; however, wind speeds only differed by about 2 mph on average.

Influence of Precipitation on Dust Release

Observations of precipitation departure from normal across the Four Corners Region suggest that the frequency and intensity of dust storms may be related to precipitation conditions during 2009 and 2017. In 2009, much of Arizona received below-average to average precipitation. This suggests that the soils across the regions were likely less saturated and therefore more prone to being picked up and transported during strong wind events. Furthermore, many of the storms during the 2009 dust season travelled through Northeastern Arizona or Northwestern New Mexico, regions with precipitation amounts that were closer to average. Accordingly, it is difficult to draw strong conclusions about the relationship between precipitation amount and the frequency and intensity of dust storms throughout the spring. However, it is possible that dust during this season was more often released from central Arizona, a region that experienced below average precipitation.

Overall, there was higher precipitation in 2017, especially over the northern portions of Utah and Southwestern part of Colorado. This aligns with CSAS data that reported above average snow water equivalent in the San Juan Mountains in 2017. By examining the maps of precipitation departure in combination with the storm trajectories for 2017 (Figure 5b), I observed that two storms travelled through the northwest corner of New Mexico, one travelled via southwest winds from northeastern Arizona, and one travelled through Southern Utah. Northern Arizona and New Mexico both received average precipitation throughout the spring, with some localized areas receiving above average precipitation. Southern Utah, for the most part, received average precipitation throughout the spring. Therefore, it is possible that the higher relative precipitation amounts received across the Colorado Plateau in 2017 might have limited the potential for dust transport throughout the season, particularly for the storms tracking through Arizona and New Mexico.

While some relationships do exist between precipitation conditions and the intensity of the dust season, there are numerous other factors that contribute to dust release including the type of vegetation or lack thereof growing on these soils. The growth of plants and other shrubs often acts as a stabilizer, whereby the roots anchor the soil. Vegetation-free areas lack that grounding source, increasingly the likelihood for dust release and transport. Second, soil type also plays a significant role in dust release. Sandier soils dry more readily than heavier textured soils, and this overall compositional difference can have ramifications for soil release or retention. Lastly, the timing of precipitation is critical for determining how likely soils will be released during strong windstorms. For example, dust is more likely to be retained when precipitation events occur during periods of strong winds, whereas moisture delivered during periods where strong winds do not occur may have already dried out by the time an event occurs that is favorable for dust transport. Accordingly, it will be important to conduct more research on the temporal connection between precipitation and dust storms in order to better understand this relationship.

Dust Deposition

In this study, I considered changes in albedo as a proxy by which to characterize dust deposition on snow, and assumed that dust-on-snow contributed to lower surface albedo. In 2017, I observed higher albedo across all four time periods, compared to 2009, where albedo values were lower overall (Figure 7). This pattern was especially evident at higher elevation locations. Mean albedo values confirm this observation, with every timepoint measuring higher mean albedo in 2017 as compared to 2009 (Table 5). Interestingly, the April 2009 map (Figure 7c) showed higher albedo in primarily lower elevation areas (left fringes of map), raising questions regarding how dust on snow might impact resulting snowmelt and extent across differing elevations. A similar pattern was observed in the May maps. This pattern could be explained by the fact that these areas likely already melted out by April, simply because of the warmer temperatures and lower snow depths at lower elevations, rather than a result of lowered albedo from dust on snow. In higher elevation areas (*e.g.,* central and Eastern parts of the map), albedo was consistently higher throughout the 2017 season as compared to 2009. Considering that dust events occurred routinely throughout this season, (1 in October, 1 in December, 1 in February, 4 in March, 5 in April) it makes sense that this dust would continue to lower albedo throughout the season despite new snowfall events. In 2017, dust storms were less frequent and less severe, meaning that this albedo remained higher over snow-covered areas. Lastly, variability in albedo across the spring, as measured by the standard deviation of albedo values, was higher in 2017 than 2009 (Table 5). This suggests that greater variation in albedo may occur in purer, less dust-affected snowpack, as compared to the snowpack of 2009 that had dust distributed throughout it and that presumably resulted in consistently lower albedo values across the extent of the study area. To enhance our understanding of this potential connection between dust and variability in albedo, future research would benefit from analyses over longer temporal periods.

Variability in snow cover during January was low in both dust years, as indicated by both the maps of NDSI (Figure 8) and associated statistics (Table 6). This aligns with expectations, as even a dust-saturated snowpack would likely still be snow covered in January due to cold temperatures and consistent snowfall. As the season proceeds to March, however, a pattern begins to form as much of the San Juan Mountains region (areas adjacent and slightly east of Silverton, Colorado) shows higher NDSI values in the 2017 season compared to 2009. This may be explained by the presence of dust storms beginning to impact snowpack extent by speeding up the melt process. This pattern was likely to have been further exacerbated due to the number and frequency of dust storms that occurred during the month of March; in 2009, 7 dust storms occurred, compared to only three in 2017. In April, lower elevation areas had, overall, higher probabilities of snow in 2009. In contrast, patterns in NDSI in higher elevation areas were similar to those observed in March, where additional dust storms likely caused faster snowpack declines in 2009 than 2017. Finally, in May, many lower elevation areas were likely already melted out, but the areas with snow still remaining had higher NDSI in 2017.

Overall, when I compared the rate of snow cover loss between the two different severity dust years, I found that 2017 followed a typical distribution for snow cover loss, with snow cover dropping by 7%, 19%, and 18% between each respective time point. A normal melt season might have shown a slightly higher drop in snow cover for the May maps; however, as 2017 was a high SWE year, these values are in line with my expectations. Snow extent decline in 2009, on the other hand, followed an entirely different pattern, with snow cover decreasing by 8%, 1%, and 32% at each respective timestep. Whereas the decline in snow extent between the March and

April NDSI maps is nearly negligible, the decline in NDSI between April and May is almost twice as high in 2009 compared to 2017. Reduced snow loss via melt earlier in the season may be explained by the comparatively colder temperatures that occurred during 2009. However, these colder than average temperatures primarily occurred later in the season and therefore do not fit the timeline of snowmelt as expected. Interestingly, 32% of snow cover was lost between April 2009 and May 2009, representing the greatest rate of decline of any timestep. This is the clearest signal of strong dust influence, whereby dust-enhanced snowmelt was triggered by dust deposition on the surface of the snowpack. The observation of exacerbated melt is also in line with the early snow-all-gone (SAG) date observed in 2009, which occurred 3 weeks earlier than in 2017 (Table 1).

Lastly, while my observations of snow extent across the season aligned with predicted behavior for a strong dust season (whereby snow cover drops significantly as dust layers are exposed, in turn exacerbating the melting process), it was more difficult to draw parallel conclusions from measures of albedo during the same time periods. I expected to observe a sharp decline in albedo between April and May 2009, consistent with the sharp decline in snow extent; however, that was not the case. Nevertheless, I did observe that albedo decreased across the entirety of the study period, which could be the result of routine dust storms that occurred throughout the season.

Future Research

This study used remote sensing to conduct a preliminary investigation into the role that dust on snow plays on surface albedo which in turn, drives snow melt. To better understand the impact of dust on snow melt out in the San Juan Mountains of Southwestern Colorado, there are several factors that should be further explored and evaluated. Firstly, the use of albedo as a proxy for dust presence inherently involves assumptions. While dust deposition undoubtedly leads to decreased albedo values, there are numerous other factors that also influence surface reflectance. For example, snowmelt can expose bare ground, vegetation, or rocks, making adjacent areas increasingly prone to melt. The presence of strong winds can also redistribute much of the deposited snow and dust, causing uneven distribution, which may significantly change the amount of snow and dust present when spring melt begins. Accordingly, future research efforts should prioritize collecting ground truthed estimates of albedo at known sites to quantify the effect of dust on snow albedo. Second, while this study pinpointed trajectories for dust storms to identify areas of dust release, more research is required to understand the exact locations where this dust originates. While inferences could potentially be drawn from remote sensing, satellite imagery is limited in its temporal resolution. Therefore, it would be useful to acquire satellite imagery collected at a higher temporal resolution in order to identify storm tracks. Alternatively, sensors placed along the trajectories of the storms identified throughout this study might be another way to make progress in this identification, and these sensors could also hypothetically measure soil mass to determine not just when the dust is being released, but also the quantity.

CONCLUSION

From the results of modeling and remote sensing analyses, I found that the greater frequency and intensity of dust storms throughout the 2009 dust season, coupled with average to below average precipitation, led to decreased albedo values throughout the spring, and also lower snow cover. This was especially pronounced in higher elevation areas, as well as in the April and May time points. However, this result was less discernible at lower elevation areas, as many of these areas do not possess snow throughout much of the spring, and are typically the first areas to melt out as the temperature warms. The statistical summaries confirmed these observations from the remotely sensed data, whereby the impact of dust was more pronounced through the latter half of spring. Uncertainty remains around the early spring of 2009, where little to no snow cover loss was observed. Future studies are crucial to better understand the impact of dust on snowpack, especially as climate change leads to fluctuating spring temperatures, more extreme winter storms, and higher variability in weather.

LITERATURE CITED

Barnett, T. P., & Pierce, D. W. (2009). *Sustainable water deliveries from the Colorado River in a changing climate* (Vol. 106, Issue 18).

Belnap, J., & Gillette, D. A. (1998). *Vulnerability of desert biological soil crusts to wind erosion: the influences of crust development, soil texture, and disturbance*.

Christensen, N. S., Wood, A. W., Voisin, N., Lettenmaier, D. P., & Palmer, R. N. (2010). *THE Effects of climate change on the hydrology and water resources of the Colorado River Basin.*

CSAS. (2009). *Red Mountain Pass SNOTEL Snowmelt Season Summary Data* .

CSAS. (2024). *Colorado Dust on Snow Program*.

Derry, J. (2017). *WY 2017 Season Summary*.

Di Mauro, B., Garzonio, R., Rossini, M., Filippa, G., Pogliotti, P., Galvagno, M., Morra Di Cella, U., Migliavacca, M., Baccolo, G., Clemenza, M., Delmonte, B., Maggi, V., Dumont, M., Tuzet, F., Lafaysse, M., Morin, S., Cremonese, E., & Colombo, R. (2019). Saharan dust events in the European Alps: Role in snowmelt and geochemical characterization. *Cryosphere*, *13*(4), 1147–1165. https://doi.org/10.5194/tc-13-1147-2019

Gautam, R., Hsu, N. C., Lau, W. K. M., & Yasunari, T. J. (2013). Satellite observations of desert dust-induced Himalayan snow darkening. *Geophysical Research Letters*, *40*(5), 988–993. https://doi.org/10.1002/grl.50226

Hammar, J., Grünberg, I., Kokelj, S. V., Van Der Sluijs, J., & Boike, J. (2023). Snow accumulation, albedo and melt patterns following road construction on permafrost, Inuvik-Tuktoyaktuk Highway, Canada. *Cryosphere*, *17*(12), 5357–5372. https://doi.org/10.5194/tc-

17-5357-2023

Hansen, J., & Nazarenko, L. (2003). *Soot climate forcing via snow and ice albedos*. www.pnas.orgcgidoi10.1073pnas.2237157100

Hock, R. (2003). Temperature index melt modelling in mountain areas. *Journal of Hydrology*, *282*(1–4), 104–115. https://doi.org/10.1016/S0022-1694(03)00257-9

Hock, R. (2005). Glacier melt: A review of processes and their modelling. In *Progress in Physical Geography* (Vol. 29, Issue 3, pp. 362–391). Arnold. https://doi.org/10.1191/0309133305pp453ra

Lawrence, C. R., Painter, T. H., Landry, C. C., & Neff, J. C. (2010). Contemporary geochemical composition and flux of aeolian dust to the San Juan Mountains, Colorado, United States. *Journal of Geophysical Research: Biogeosciences*, *115*(3). https://doi.org/10.1029/2009JG001077

Liang, S. (2000). *Narrowband to broadband conversions of land surface albedo I Algorithms*. www.elsevier.com/locate/rse

Naegeli, K., Damm, A., Huss, M., Wulf, H., Schaepman, M., & Hoelzle, M. (2017). Cross-Comparison of Albedo Products for Glacier Surfaces Derived from Airborne and Satellite (Sentinel-2 and Landsat 8) Optical Data. *Remote Sensing*, *9*(2), 110. https://doi.org/10.3390/rs9020110

Neff, J. C., Ballantyne, A. P., Farmer, G. L., Mahowald, N. M., Conroy, J. L., Landry, C. C., Overpeck, J. T., Painter, T. H., Lawrence, C. R., & Reynolds, R. L. (2008). Increasing eolian dust deposition in the western United States linked to human activity. *Nature Geoscience*, *1*(3), 189–195. https://doi.org/10.1038/ngeo133

Neff, J. C., Reynolds, R. L., Munson, S. M., Fernandez, D., & Belnap, J. (2013). The role of dust storms in total atmospheric particle concentrations at two sites in the western U.S. *Journal of Geophysical Research Atmospheres*, *118*(19), 11,201-11,212. https://doi.org/10.1002/jgrd.50855

Oerlemans, J. (2000). Analysis of a 3 year meteorological record from the ablation zone of morteratschgletscher, Switzerland: Energy and mass balance. *Journal of Glaciology*, *46*(155), 571–579. https://doi.org/10.3189/172756500781832657

Okin, G. S. (2022). Where and How Often Does Rain Prevent Dust Emission? *Geophysical Research Letters*, *49*(4). https://doi.org/10.1029/2021GL095501

Painter, T. H., Barrett, A. P., Landry, C. C., Neff, J. C., Cassidy, M. P., Lawrence, C. R., McBride, K. E., & Farmer, G. L. (2007). Impact of disturbed desert soils on duration of mountain snow cover. *Geophysical Research Letters*, *34*(12). https://doi.org/10.1029/2007GL030284

Painter, T. H., Skiles, S. M. K., Deems, J. S., Brandt, W. T., & Dozier, J. (2018). Variation in Rising Limb of Colorado River Snowmelt Runoff Hydrograph Controlled by Dust Radiative Forcing in Snow. *Geophysical Research Letters*, *45*(2), 797–808. https://doi.org/10.1002/2017GL075826

Skiles, S. M. K., & Painter, T. (2017). Daily evolution in dust and black carbon content, snow grain size, and snow albedo during snowmelt, Rocky Mountains, Colorado. *Journal of Glaciology*, *63*(237), 118–132. https://doi.org/10.1017/jog.2016.125

Skiles, S. M. K., Painter, T. H., Deems, J. S., Bryant, A. C., & Landry, C. C. (2012). Dust radiative forcing in snow of the Upper Colorado River Basin: 2. Interannual variability in radiative forcing and snowmelt rates. *Water Resources Research*, *48*(7). https://doi.org/10.1029/2012WR011986

Skiles, S. M., Painter, T. H., Belnap, J., Holland, L., Reynolds, R. L., Goldstein, H. L., & Lin, J. (2015). Regional variability in dust-on-snow processes and impacts in the Upper Colorado River Basin. *Hydrological Processes*, *29*(26), 5397–5413. https://doi.org/10.1002/hyp.10569

Stein, A. F., Draxler, R. R., Rolph, G. D., Stunder, B. J. B., Cohen, M. D., & Ngan, F. (2015). Noaa's hysplit atmospheric transport and dispersion modeling system. In *Bulletin of the American Meteorological Society* (Vol. 96, Issue 12, pp. 2059–2077). American Meteorological Society. https://doi.org/10.1175/BAMS-D-14-00110.1